Article

Cell Stem Cell

Tex10 Coordinates Epigenetic Control of Super-Enhancer Activity in Pluripotency and Reprogramming

Graphical Abstract

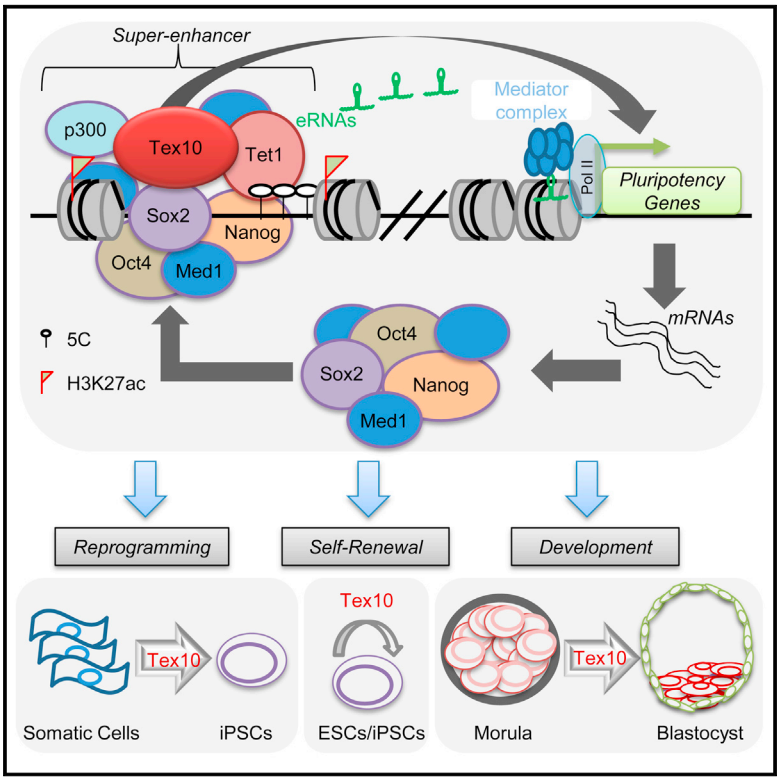

Authors

Junjun Ding, Xin Huang, ..., Xiaohua Shen, Jianlong Wang

Correspondence

jianlong.wang@mssm.edu

In Brief

Using Sox2-centered interactome analysis, Ding et al. identify Tex10 as an evolutionarily conserved key pluripotency factor that plays a critical role in ESC self-renewal and pluripotency, early embryo development, and somatic cell reprogramming via epigenetic regulation of super-enhancer activity.

Highlights

- Interactome analysis highlights Tex10 as a binding partner of Sox2
- Tex10 is required for maintenance and establishment of pluripotency
- Tex10 regulates super-enhancer activity via epigenetic modifications
- Sox2 targets Tex10 to ESC-specific super-enhancers

Accession Numbers

GSE66736

Ding et al., 2015, Cell Stem Cell *16*, 653–668
June 4, 2015 ©2015 Elsevier Inc.
http://dx.doi.org/10.1016/j.stem.2015.04.001

Cell Stem Cell
Article

Tex10 Coordinates Epigenetic Control of Super-Enhancer Activity in Pluripotency and Reprogramming

Junjun Ding,[1,3] Xin Huang,[1,3] Ningyi Shao,[4] Hongwei Zhou,[1,3] Dung-Fang Lee,[1,3] Francesco Faiola,[1,3] Miguel Fidalgo,[1,3] Diana Guallar,[1,3] Arven Saunders,[1,2,3] Pavel V. Shliaha,[5] Hailong Wang,[6] Avinash Waghray,[1,2,3] Dmitri Papatsenko,[1,3] Carlos Sánchez-Priego,[1,3] Dan Li,[1,2,3] Ye Yuan,[1,2,3] Ihor R. Lemischka,[1,2,3,7] Li Shen,[4] Kevin Kelley,[3] Haiteng Deng,[8] Xiaohua Shen,[8] and Jianlong Wang[1,2,3,*]

[1]The Black Family Stem Cell Institute, Icahn School of Medicine at Mount Sinai, New York, NY 10029, USA
[2]The Graduate School of Biomedical Sciences, Icahn School of Medicine at Mount Sinai, New York, NY 10029, USA
[3]Department of Developmental and Regenerative Biology, Icahn School of Medicine at Mount Sinai, New York, NY 10029, USA
[4]Fishberg Department of Neuroscience and Friedman Brain Institute, Icahn School of Medicine at Mount Sinai, New York, New York 10029, USA
[5]Department of Biochemistry, University of Cambridge, Tennis Court Road, Cambridge, CB21QR, UK
[6]Organ Transplantation Institute, Xiamen University, Xiamen City, Fujian Province 361102, China
[7]Department of Pharmacology and Systems Therapeutics, Icahn School of Medicine at Mount Sinai, New York, NY 10029, USA
[8]Tsinghua-Peking Center for Life Sciences, School of Medicine, Tsinghua University, Beijing 100084, China
*Correspondence: jianlong.wang@mssm.edu
http://dx.doi.org/10.1016/j.stem.2015.04.001

SUMMARY

Super-enhancers (SEs) are large clusters of transcriptional enhancers that are co-occupied by multiple lineage-specific transcription factors driving expression of genes that define cell identity. In embryonic stem cells (ESCs), SEs are highly enriched for the core pluripotency factors Oct4, Sox2, and Nanog. In this study, we sought to dissect the molecular control mechanism of SE activity in pluripotency and reprogramming. Starting from a protein interaction network surrounding Sox2, we identified Tex10 as a key pluripotency factor that plays a functionally significant role in ESC self-renewal, early embryo development, and reprogramming. Tex10 is enriched at SEs in a Sox2-dependent manner and coordinates histone acetylation and DNA demethylation at SEs. Tex10 activity is also important for pluripotency and reprogramming in human cells. Our study therefore highlights Tex10 as a core component of the pluripotency network and sheds light on its role in epigenetic control of SE activity for cell fate determination.

INTRODUCTION

Transcription factors (TFs) regulate tissue-specific gene expression programs through interactions with enhancer elements (Buecker et al., 2014). Compared with typical enhancers (TEs), super-enhancers (SEs) are large clusters of transcriptional enhancers that drive expression of genes that define cell identity. In ESCs, SEs are highly enriched for Oct4, Sox2, and Nanog (OSN) (Whyte et al., 2013) and express a group of non-coding RNAs known as eRNAs (Lam et al., 2014), although the mechanisms by which pluripotency factors regulate SE activity and eRNA transcription are not well defined. Enhancer activation requires the presence of multiple lineage-specific TFs and TF-recruited coactivators such as CBP/p300 (Chen et al., 2008), which together help to establish the histone marks of active enhancers such as H3K4me1 and H3K27ac. Active enhancers are also bound by general TFs and RNA polymerase II (Pol II), leading to the production of eRNAs in SEs, and to a lesser extent, in TEs (Hnisz et al., 2013). The eRNAs are transcribed from Tet-occupied, hypomethylated enhancers (Pulakanti et al., 2013) and are able to mediate gene activation (Lam et al., 2014). It is poorly defined how pluripotency TFs and their associated cofactors may transcriptionally regulate the expression of SE eRNAs to maintain the pluripotent identity of ESCs.

Studies of Nanog (Costa et al., 2013; Wang et al., 2006) and Oct4 (Ding et al., 2012; Pardo et al., 2010; van den Berg et al., 2010) interactomes in ESCs have led to the discovery of many novel pluripotency TFs and associated epigenetic regulators (Huang and Wang, 2014) that play important roles in maintaining pluripotency and promoting reprogramming. In contrast, studies of Sox2-associated protein complexes have only been performed in early differentiating ESCs (Mallanna et al., 2010) or in a transgenic ESC line expressing all four "Yamanaka reprogramming factors" (Gao et al., 2012), leaving it an open question of whether the bona fide Sox2 interactome has been identified. Consequently, additional transcription cofactors and/or epigenetic regulators that are required for Sox2 to target and exert transcriptional regulation of target genes remain to be defined. Whereas Sox2 co-occupies ESC TEs and SEs with Nanog, Oct4, and Mediator in maintaining ESC identity (Hnisz et al., 2013; Kagey et al., 2010; Whyte et al., 2013), it directly interacts only with Nanog (Gagliardi et al., 2013) while relying on DNA for its Oct4 association (Lam et al., 2012). Sox2 binds first to the predominant Sox2/Oct4 co-binding motif, defined as the *Sox-Oct* enhancer, which is followed by assisted binding of Oct4 during the enhanceosome assembly in ESCs (Chen et al., 2014).

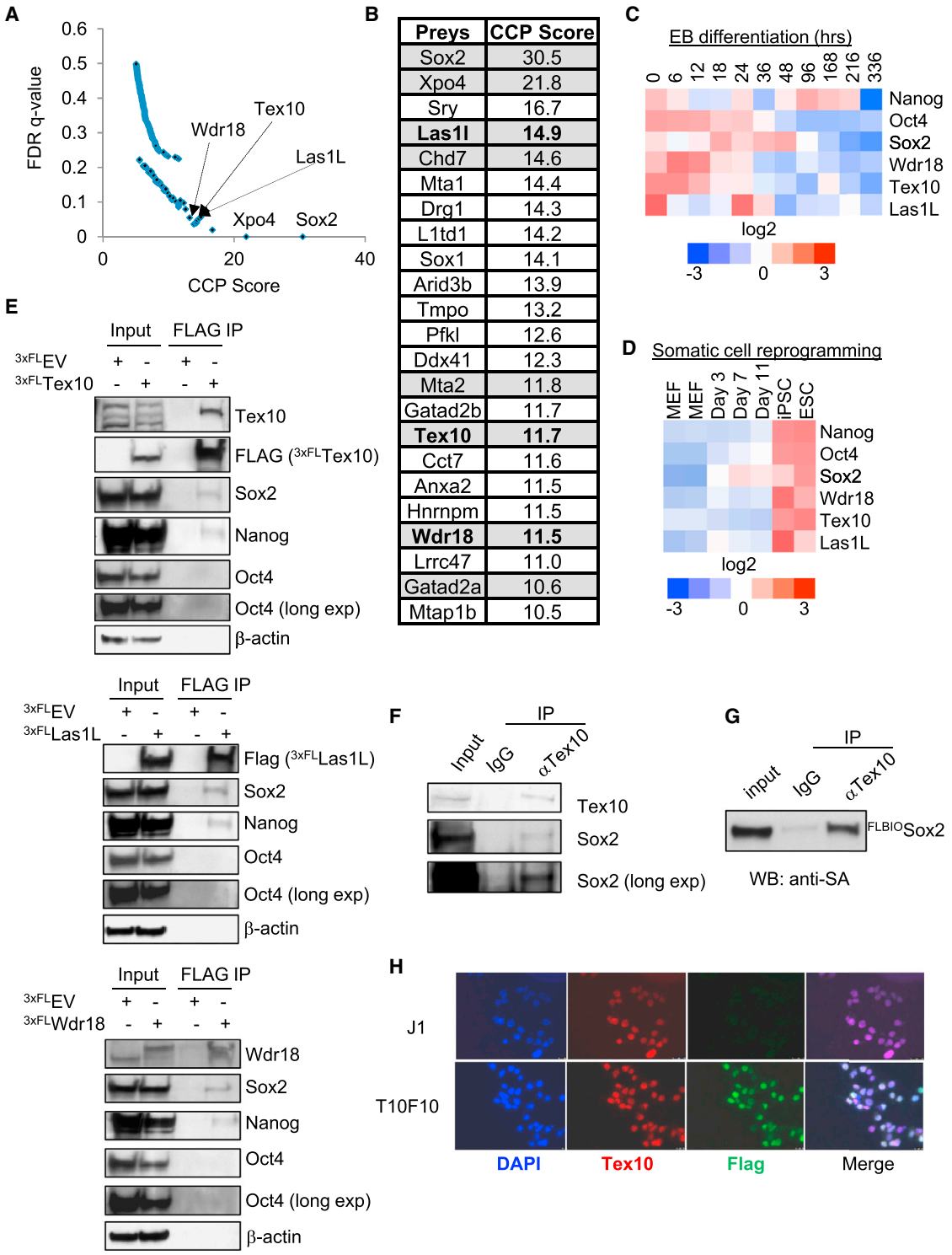

Preys	CCP Score
Sox2	30.5
Xpo4	21.8
Sry	16.7
Las1l	**14.9**
Chd7	14.6
Mta1	14.4
Drg1	14.3
L1td1	14.2
Sox1	14.1
Arid3b	13.9
Tmpo	13.2
Pfkl	12.6
Ddx41	12.3
Mta2	11.8
Gatad2b	11.7
Tex10	**11.7**
Cct7	11.6
Anxa2	11.5
Hnrnpm	11.5
Wdr18	**11.5**
Lrrc47	11.0
Gatad2a	10.6
Mtap1b	10.5

Figure 1. Identification of Wdr18, Tex10, and Las1L as Novel Partners of Sox2

(A) All proteins (one dot shows one protein) are shown by combined cumulative probability (CCP) scores and FDR q values.

(B) List of 23 preys with highest CCP scores. The proteins were selected by a cut-off of $q < 0.10$ and CCP > 10.5.Validated interactions by a previous study (Gao et al., 2012) or in this study by IP/co-IP are shaded in gray. Wdr18, Tex10, and Las1L are in bold text.

(C) Gene expression of *Wdr18*, *Tex10*, and *Las1L* during EB differentiation. Microarray data are from GEO: GSE3749. The scale represents fold changes.

(D) Gene expression of *Wdr18*, *Tex10*, and *Las1L* during somatic cell reprogramming. Microarray data are from GEO: GSE19023. The scale represents fold changes.

(E) Validation of physical associations of Wdr18, Tex10, and Las1L with Oct4, Sox2, and Nanog by co-IP in J1 ESCs.

(legend continued on next page)

Interestingly, endogenous *Sox2* is also hierarchically activated first in the deterministic stage of reprogramming and plays an important role in orchestrating downstream pluripotency gene activation, including that of *Oct4* and *Nanog*, during the establishment of pluripotency (Buganim et al., 2012; Polo et al., 2012). Therefore, identification of additional Sox2 cofactors and epigenetic regulators that play critical roles in pluripotency and reprogramming will greatly facilitate a better understanding of Sox2-guided enhanceosome assembly in ESCs, and in particular, SE control for the pluripotent cell identity.

We employed immunoprecipitation (IP) for affinity purification of Sox2 protein complexes in ESCs combined with mass spectrometry (MS) to construct an extended Sox2 interactome for identification of such important factors. Here we report our discovery of Tex10 as a bona fide Sox2 partner and critical pluripotency factor with a unique mode of action in controlling SE activity via modulating DNA methylation and histone acetylation for stem cell maintenance, somatic cell reprogramming, and early embryogenesis. Specifically, we found that Tex10 is critically required for both maintenance of ESCs and establishment of pluripotency during early embryogenesis and somatic cell reprogramming. Mechanistically, Tex10 recruits the coactivator histone acetyltransferase p300 and cooperates with DNA hydroxylase Tet1 for epigenetic modifications of the SEs associated with pluripotency gene loci. Consequently, H3K27 acetylation and hypomethylation of SEs lead to enhanced eRNA transcription and positive regulation of pluripotency gene expression. Finally, we demonstrate the functional conservation of this key pluripotency factor in both mouse and human pluripotency.

RESULTS

The Sox2 Interactome Identifies Tex10 as an Interacting Partner of Sox2

Following our well-established protocols (Costa et al., 2013; Ding et al., 2012) for affinity purification in mouse ESCs (Figures S1A–S1E, and see Experimental Procedures for details) and employing an iPAC algorithm for interactome analysis (see Supplemental Experimental Procedures for details), we identified 67 high confidence Sox2-interacting proteins (Table S1; Figures 1A and S1F). These contain many TFs, RNA processing factors, protein folding factors, epigenetic regulators, and others (Figure S1F). The top 23 proteins as the highest confidence candidates for Sox2 partners are identified with the most stringent cut-off false discovery rate (FDR) and combined cumulative probability (CCP) scores (Figure 1B and see Supplemental Experimental Procedures). These include factors whose interactions with Sox2 were either previously reported (e.g., Xpo4; Gontan et al., 2009) or newly confirmed (e.g., Chd7; Figure S1G) (shaded gray in Figure 1B). Our Sox2 interactome contains both documented (e.g., NuRD proteins) and potentially novel (see below) ESC regulators that play important roles in pluripotency (Hu and Wade, 2012) and reprogramming (Dos Santos et al., 2014; Rais et al., 2013).

We were particularly interested in the newly identified Sox2 partners Wdr18, Tex10, and Las1L for several reasons. First, all three factors are often co-purified as part of the 5FMC (five friends of methylated Chtop) (Fanis et al., 2012), MLL1/MLL (Dou et al., 2005), and Rix (Castle et al., 2012) complexes in other cellular systems, which play such important roles as linking arginine methylation to desumoylation for transcriptional regulation, modifying H3K4 methylation, and controlling ribosome biogenesis and cell cycle regulation through p53, respectively. Cell cycle control has been intrinsically linked with pluripotency and reprogramming (Hindley and Philpott, 2013) and ribosome biogenesis is being recognized for its potential role in controlling pluripotency and reprogramming (Fong et al., 2014) and germline stem cell fate (Zhang et al., 2014). Second, they are all highly enriched in ESCs and are downregulated during embryoid body (EB) differentiation (Figure 1C) or in non-pluripotent cells (Figure S1I). Third, they are all upregulated during the generation of induced pluripotent stem cells (iPSCs) (Figure 1D). Such expression patterns mimic those of the core pluripotency factors OSN (Figures 1C and 1D). Fourth, all three factors interact with Sox2 and Nanog, but less likely with Oct4 (Figures 1E and S1J), which is consistent with them being Sox2 partners and the association of Sox2 with Nanog being direct (Gagliardi et al., 2013), whereas the association with Oct4 is DNA dependent (Lam et al., 2012). Taken together, our data and published studies suggest that these three factors may play important roles in controlling pluripotency and reprogramming.

In summary, we have established an extended Sox2 interactome and identified 23 high confidence Sox2 partners that have known or potential roles in controlling pluripotency and reprogramming. Our study thus provides a rich resource for further dissecting Sox2-guided enhanceosome assembly and particularly the dynamic control of SE activity for the pluripotent cell identity in ESC maintenance and iPSC generation.

Tex10 Is Required for Self-Renewal and Pluripotency of ESCs

We focused on Tex10 to dissect the dynamic control of Sox2-guided enhanceosome assembly and understand its roles in pluripotency and reprogramming. We first confirmed the endogenous interaction between Tex10 and Sox2 (Figures 1F and 1G and S1H) and demonstrated that Tex10 is a nuclear protein highly expressed in ESCs (Figure 1H), although mRNA expression levels are also enriched in several adult mouse tissues such as testis, uterus, and lung (Figure S1K). We then performed loss-of-function experiments to study the potential roles for Tex10 in ESC maintenance. Downregulation of *Tex10* with two independent shRNAs (Figure 2A) resulted in the reduction of total colony number and size with an increased proportion of partially and fully differentiated populations and reduced alkaline phosphatase (AP) activity (Figures 2B and 2C), indicating the loss of

(F) Validation of the endogenous interaction between Sox2 and Tex10 by Tex10 antibody-based IP in CCE ESCs.
(G) Validation of the Sox2-Tex10 interaction by Tex10 antibody-based IP in ESCs expressing the ^{FLBIO}*Sox2* transgene.
(H) Immunofluorescence staining of Tex10 (red) and FLAG (green) in J1 and T10F10 (J1 with ectopic ^{3xFL}*Tex10* expression) ESCs. Cell nuclei were counter-stained with DAPI (blue).
See also Figure S1.

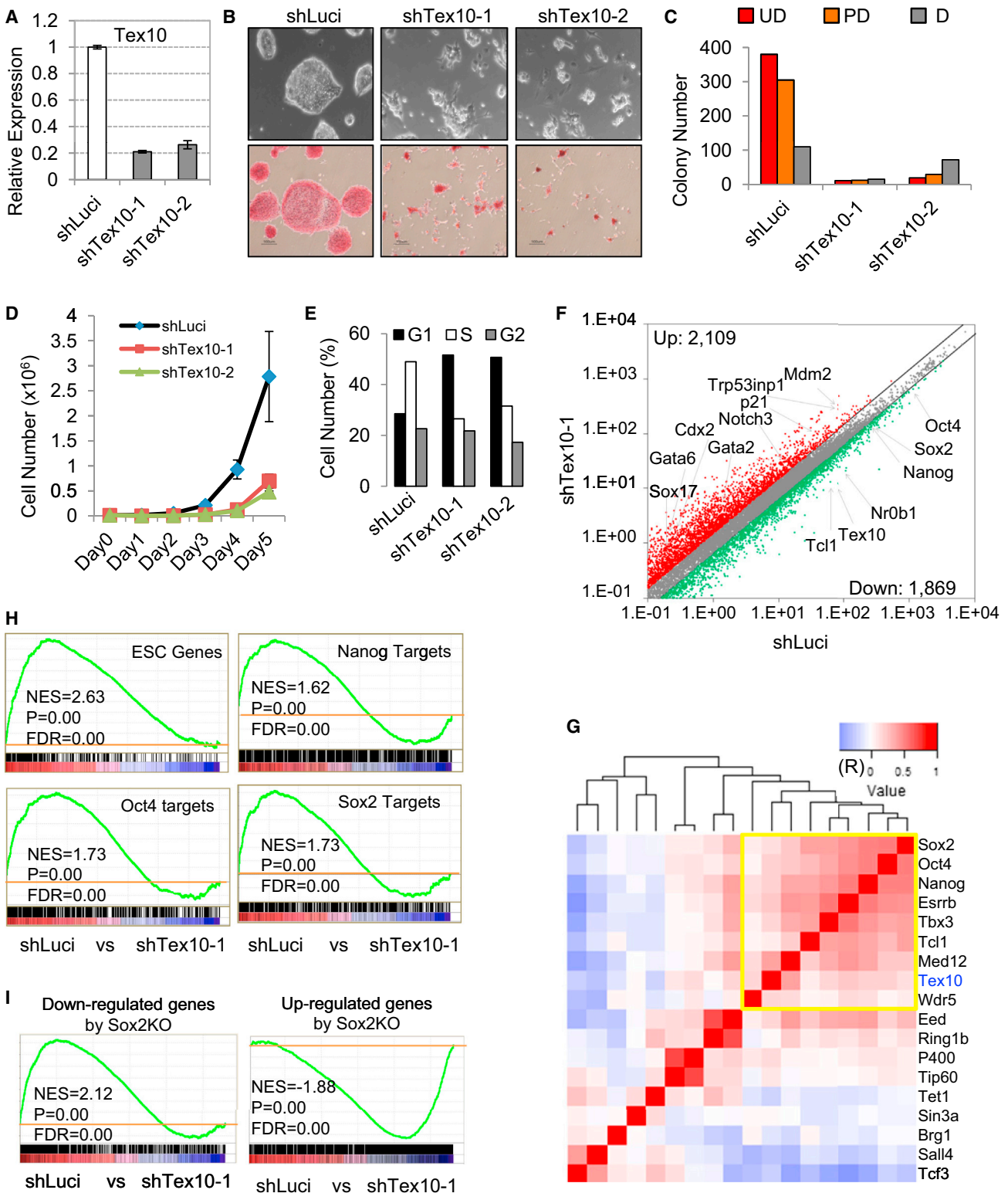

Figure 2. Tex10 Is Required for ESC Maintenance

(A) Quantitative PCR analysis of *Tex10* expression after 4 days of *Tex10* knockdown. Data are presented as mean ± SEM (n = 3).

(B) Morphology of *Tex10* knockdown ESCs with (bottom) or without (top) AP staining.

(C) Colony formation assay for ESCs with *luciferase* (*Luci*) knockdown or *Tex10* knockdwon. Individual colonies were stained for AP activity and scored into three categories (UD, uniformly undifferentiated; PD, partially differentiated or mixed; and D, differentiated) as indicated.

(legend continued on next page)

self-renewal. Consistent with this, *Tex10*-depleted ESCs grew slower than control ESCs (Figure 2D) due to an elongated G1 phase (Figure 2E) and not to apoptosis (Figure S2A). Such a defect in self-renewal can be rescued by ectopic expression of a *Tex10* transgene that lacks the shRNA target site, excluding off-target effects of the shRNAs (Figures S2B and S2C). Of note, a similar requirement of the core pluripotency factors OSN for efficient G1/S transition in both human (Card et al., 2008; Zhang et al., 2009) and mouse (Schoeftner et al., 2013) ESCs has also been reported, suggesting a potential functional interaction between Tex10 and OSN.

To further understand how Tex10 regulates self-renewal at the molecular level, we performed RNA-seq analyses in control *luciferase* knockdown and *Tex10* knockdown cells, which led to the identification of 1,869 and 2,109 genes that are downregulated and upregulated, respectively, upon *Tex10* depletion (Figures 2F and S2D). More importantly, the downregulated and upregulated genes correspond to those that are highly enriched in ESCs and differentiated cells of multiple lineages including the trophoblast lineage (Figures S2D–S2F). Supporting the fact that Tex10 may globally intersect with the pluripotency transcription network for ESC maintenance, we found a close correlation of the transcriptomic changes upon *Tex10* depletion with those upon depletion of other pluripotency factors including *OSN*, *Esrrb*, and *Tbx3* (Figure 2G, yellow square). In addition, *Tex10* depletion reduced the expression of ESC-enriched genes as well as the targets of OSN (Figure 2H). Finally, the global expression profile induced by *Tex10* knockdown is significantly similar to that resulting from *Sox2* depletion (Figure 2I), further confirming that Tex10 not only physically but also functionally interacts with Sox2 in maintaining pluripotency.

Together, our data indicate that Tex10 is a previously unappreciated factor that functionally intersects with the core pluripotency network for optimal self-renewal and pluripotency of ESCs, establishing Tex10 as a key pluripotency factor.

Tex10 Is Required for Early Mouse Development

We reasoned that Tex10 as a key pluripotency factor must also be critical for mouse early development. Single-cell transcriptomic analysis of early mouse embryos (Tang et al., 2011) revealed that *Tex10* mRNA is upregulated during embryonic development from oocyte to inner cell mass (ICM) stages, although it is also expressed in trophectoderm and slightly downregulated in epiblast (Figure 3A). Established ESCs have further enhanced *Tex10* expression (Figure 3A). Such an expression pattern during early embryo development was further confirmed by LacZ staining of *Tex10* heterozygous mouse embryos harboring a gene trap allele (Figure S3A) at corresponding stages (Figure 3B). Consistent with the biochemical evidence on the Sox2-Tex10 partnership (Figure 1), we also found co-localization of these two proteins in mouse blastocysts (Figure 3C), supporting the physical and functional connection of Tex10 and Sox2 both in vitro and in vivo.

To directly test the function of Tex10 during early embryo development, we injected siRNA against *Tex10* (si*Tex10*) and non-targeting control (si*Non*) into wild-type (from mating C57Bl/6J with C57Bl/6J×DBA/2J, or B6D2) mouse zygotes and then cultured those embryos in vitro. We found that depletion of *Tex10* significantly reduced the embryo development from morula to blastocyst stage (Figures 3D and 3E and S3B). We confirmed efficient knockdown of *Tex10* and also noticed a reduction of *Sox2* expression as well as upregulation of *p53* and its direct downstream target *p21* (Figure 3F). A similar effect of *Tex10* depletion on Sox2, p53, and p21 was also observed in ESCs at both the protein (Figure S2G) and transcript (Figures 2F and S2H) levels. Since knockdown of *p53* only partially rescues the defects of cell cycle, proliferation, and self-renewal of *Tex10*-depleted ESCs (Figures S2I–S2L), we believe that a combined effect of downregulation of pluripotency genes (e.g., *Sox2*) and upregulation of *p53* and *p21* may have contributed to compromised early embryo development.

To further investigate the role of Tex10 during mouse development, we created a *Tex10* knockout mouse model by using $Tex10^{+/LacZ}$ ESCs (Figures S3A and S3C). We successfully obtained heterozygous males and females that are phenotypically normal with a regular life span. Among 95 pups generated from matings between heterozygous males and females, we obtained 25 wild-type and 70 heterozygous $Tex10^{+/LacZ}$ mice, but no homozygous mutants ($Tex10^{LacZ/LacZ}$) (Figure 3G), indicating that *Tex10* homozygous pups may have died before birth. We thus performed early embryo analyses by examining 39 decidual swellings obtained at mid-gestation 7.5 dpc, among which we found 15 empty deciduas, 6 wild-type embryos, and 16 heterozygous embryos, as well as 2 embryos of unknown genotype (with such a designation due to limited material) (Figure 3H). These data suggest that *Tex10* knockout is likely early embryonic lethal prior to 7.5 dpc, which is consistent with our siRNA experiment demonstrating the morula-to-blastocyst arrested phenotype (Figures 3D and 3E and S3B). To further corroborate this, we attempted to derive ESCs from 3.5 dpc blastocysts obtained from heterozygous matings (Figure S3C). A total of 54 blastocysts were obtained for outgrowth following standard protocol (Meissner et al., 2009), among which 27 colonies were grown out and the other half failed to grow due to technical difficulties and/or presumed mutant consequences. Among the 27 outgrown colonies, 17 were stably established for genotyping

(D) Growth curve analysis of *Tex10*-depleted ESCs. *Luciferase* knockdown (*shLuci*) serves as a control. Data are presented as mean ± SEM (n = 3).
(E) Cell cycle analysis of *Tex10*-depleted ESCs. *Luciferase* knockdown (*shLuci*) serves as a control.
(F) Scatter plot of the RNA-seq expression data from *luciferase* and *Tex10* knockdown ESCs.
(G) Hierarchical clustering of pluripotency factors based on transcriptome changes upon depletion of each individual factor. The scale represents a Pearson correlation coefficient (R).
(H) Gene set enrichment analysis of the RNA-seq data from *luciferase* and *Tex10* knockdown ESCs. Sets of the ESC-enriched genes (Ben-Porath et al., 2008) and the targets of Nanog, Sox2, and Oct4 (Ang et al., 2011; Lee et al., 2012) are used.
(I) Gene set enrichment analysis of the RNA-seq data from *luciferase* and *Tex10* knockdown ESCs. Sets of the downregulated and upregulated genes at 72 hr after *Sox2* knockout (GEO: GSE5895) are used.
See also Figure S2.

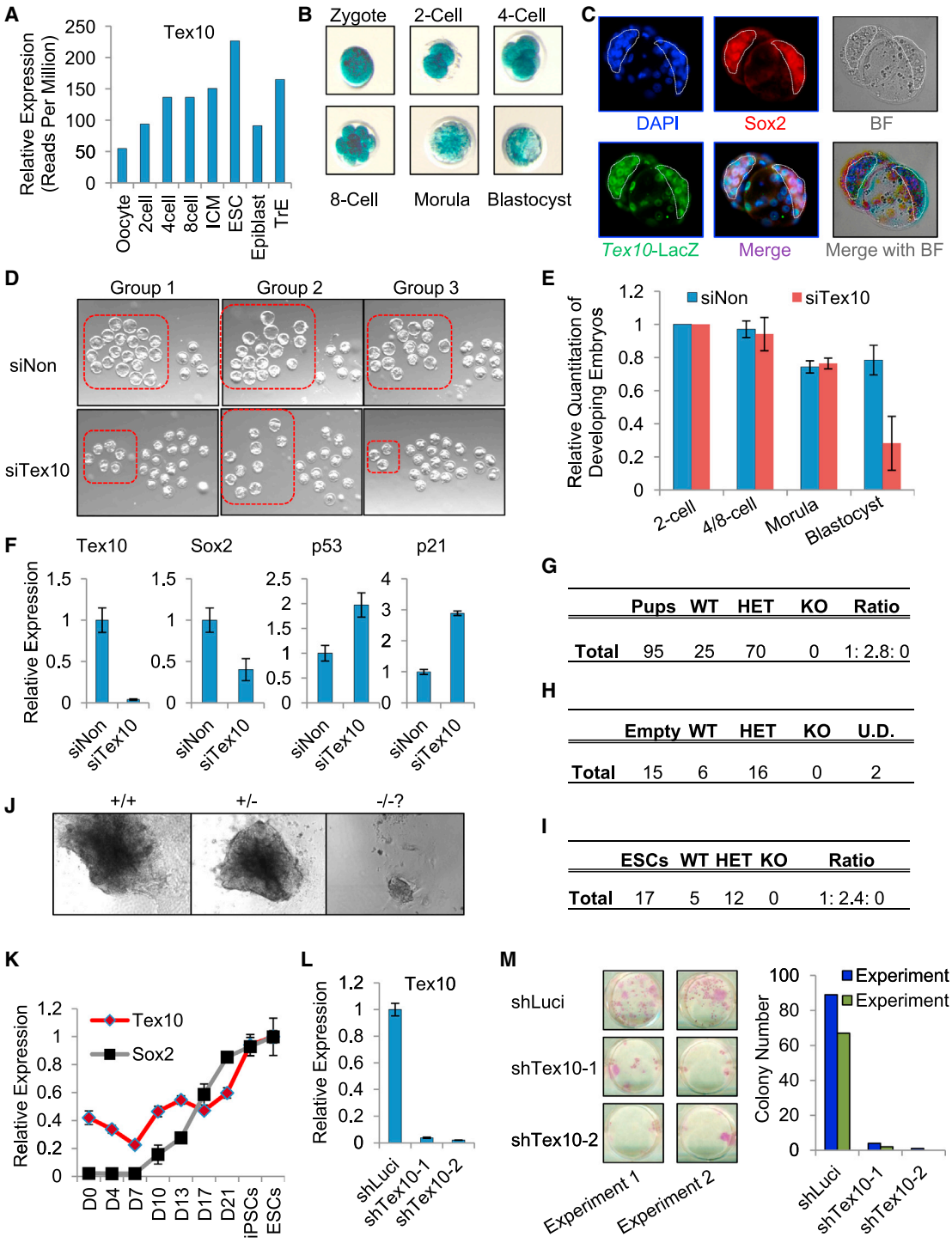

Figure 3. Tex10 Plays Critical Roles in the Establishment of Pluripotency In Vivo and In Vitro

(A) *Tex10* expression during early embryonic development based on published dataset (GEO: GSE22182). ICM, inner cell mass; TrE, trophectoderm.

(B) X-gal staining of early embryos. The gene trap allele of *Tex10* expressing LacZ was depicted in Figure S3A.

(C) Immunofluorescence staining of LacZ (driven by the *Tex10* promoter) (green) and Sox2 (red) in two overlapping blastocysts. Cell nuclei were counter-stained with DAPI (blue). ICM is encircled with a dotted line for each blastocyst.

(D) Effect of *Tex10* knockdown on blastocyst development. Zygotes were arbitrarily separated into three groups and processed in parallel for siRNA treatments and morphological examinations. Morphology of embryos 4.5 days after siRNA injection is shown. The normal developing blastocysts are shown in red rectangles.

(legend continued on next page)

(Figures 3I and 3J), revealing 5 wild-type and 12 heterozygous (Figure 3I) lines of typical ESC colony morphology (Figure 3J, left and middle panels). The remaining 10 initially grew but then could not be further propagated for genotyping and were presumed mutants (Figure 3J, the right panel). These results suggest that *Tex10* null embryos may not develop to the blastocyst stage and/or that mutant blastocysts are defective for in vitro ICM outgrowth.

Together, our data functionally define Tex10 as a key pluripotency factor that is essential for early development, although the exact cause of early embryonic lethality of *Tex10* knockouts and its potential roles in trophectoderm (Figures 3A–3C) and testis (Figure S1K) remain the subject for future investigation with a conditional null allele.

Tex10 Is Required for Efficient Somatic Cell Reprogramming

We explored the potential roles for Tex10 in the establishment of pluripotency during somatic cell reprogramming. We first tested knockdown or ectopic expression of *Tex10* in conventional Yamanaka reprogramming of mouse embryonic fibroblasts (MEFs) (Figure S3D). Like *Sox2*, *Tex10* is activated during the late stage of reprogramming (Figure 3K). Consistent with the crucial roles of Sox2 in orchestrating the transcriptional activation hierarchy at this stage (Buganim et al., 2012; Polo et al., 2012), we found that knockdown of *Tex10* (Figure 3L), a close partner of Sox2, also dramatically decreased MEF reprogramming efficiency (Figure 3M). This reprogramming defect upon *Tex10* depletion is minimally attributed to decreased MEF proliferation (Figures S3E and S3F), but more likely to a combinatorial effect of compromised mesenchymal-to-epithelial transition (Figures S3H–S3J) and the reduced reactivation of pluripotency genes during reprogramming (Figure S3K). Conversely, ectopic expression of *Tex10* enhanced the reprogramming efficiency by 6-fold (Figure S3G), although it cannot replace *Sox2* in reprogramming (data not shown).

To directly address Tex10 function in the final stage of reprogramming, we employed the Nanog-driven pre-iPSC reprogramming system (Silva et al., 2008) (Figure S3L). Like *Sox2*, *Tex10* is also activated at the final stage during pre-iPSC reprogramming (Figure S3M). Depletion of *Tex10* reduced Nanog-driven reprogramming efficiency compared with the empty vector control as measured by *Oct4*-GFP-positive colony numbers (Figure S3N). Together with the data presented in Figure 2, our study establishes a critical role of Tex10 for both the maintenance and establishment of pluripotency in vitro and in vivo.

Tex10 Positively Regulates SE Activity

To understand the molecular mechanisms by which Tex10 regulates pluripotency, we identified global genomic targets of Tex10 by chromatin IP (ChIP)-seq in ESCs ectopically expressing 3×FLAG-tagged Tex10. Owing to the lack of a ChIP-grade Tex10 antibody, FLAG antibody-based ChIP was performed and specific enrichment of Tex10 in FLAG ChIPed samples was confirmed by Tex10 western blot, validating the FLAG ChIP for detecting Tex10 binding DNA fragments (Figure S4A). A total of 5,189 Tex10 binding regions (peaks) were identified, among which 47.8%, 32.3%, and 19.9% of peaks are localized in promoters, intergenic regions, and gene bodies, respectively (Figure 4A). Consistent with the high percentage of promoter occupancy, Tex10 peaks are enriched at transcription start sites (TSSs) (Figure S4B). Since Tex10 is physically associated with Sox2, as expected, we found that 46% of Tex10 targets are also bound by Sox2 (Figure S4C) and that the Tex10 binding motif (de novo) is significantly similar to the Sox2 binding consensus motif (Figure S4D; $p = 10^{-238}$). Such a strong correlation of genomic localization with Sox2 was shared by other pluripotency factors such as Nanog, Oct4, Med1/12, and Esrrb (Figure S4E). We also found Tex10 clustered together with OSN and Med1/12 at a global level in target gene occupancy (Figure S4F, red and green rectangles). Combined with the RNA-seq data (Figure 2F), we found that *Tex10* knockdown significantly reduced the expression of the genes within 5 kb of Tex10 binding regions (Figure S4G), indicating that Tex10 is a positive regulator of gene expression in ESCs. These results strongly support that Tex10 is an integral part of the core pluripotency network encompassing OSN that governs the ESC identity.

Active ESC enhancers are often co-occupied by multiple core pluripotency factors including OSN and are marked with high levels of H3K4me1 and H3K27ac in combination with a low level of H3K4me3 (Creyghton et al., 2010; Kagey et al., 2010). Interestingly, we found that Tex10 binding regions are also enriched for OSN (Figure 4B) as well as the active enhancer marks (H3K4me1 and H3K27ac) (Figure 4C), suggesting that Tex10, as a close partner of Sox2, may play a role in Sox2-guided enhanceosome assembly regulating enhancer activity in ESCs. We selected the enhancers by these histone marks and beyond 3 kb of TSS, revealing that Tex10 is indeed enriched at enhancer regions (Figure 4D). While Tex10-only binding regions are low in H3K4me1 (Figure 4E; blue bars) and high in H3K27ac (Figure 4E; yellow bars), Tex10 and Sox2 co-binding regions are greatly enriched for the combination of both marks (H3K4me1+H3K27ac) (Figure 4E, red bars), suggesting a Sox2-dependent function of

(E) Relative quantitation of normal embryos at each developmental stage. Values were normalized to the two-cell stage and plotted as mean ± SEM from three independent groups shown in (D).
(F) Gene expression analysis by RT-qPCR in the si*Tex10*-injected morulas relative to si*Non* controls. Expression is normalized by Gapdh and data are presented as mean ± SEM (n = 3).
(G) Table summarizing the live born litter and Mendelian ratio of mice from $Tex10^{+/-}$ × $Tex10^{+/-}$ matings.
(H) Table summarizing 7.5 dpc embryos from $Tex10^{+/-}$ × $Tex10^{+/-}$ matings. U.D., undetermined.
(I) Table summarizing genotypes and Mendelian ratio of established ESC lines from outgrowth of blastocysts derived from $Tex10^{+/-}$ × $Tex10^{+/-}$ matings.
(J) Morphology of established ESCs as summarized in (I).
(K) Expression of *Tex10* and *Sox2* during MEF reprogramming. Data are presented as mean ± SEM (n = 3).
(L) Knockdown efficiency of *Tex10* shRNA in MEFs.
(M) Compromised reprogramming efficiency of MEFs upon *Tex10* depletion compared with *luciferase* knockdown. AP staining (left) and quantitation (right) of AP-positive colony numbers from two independent experiments are shown.
See also Figure S3.

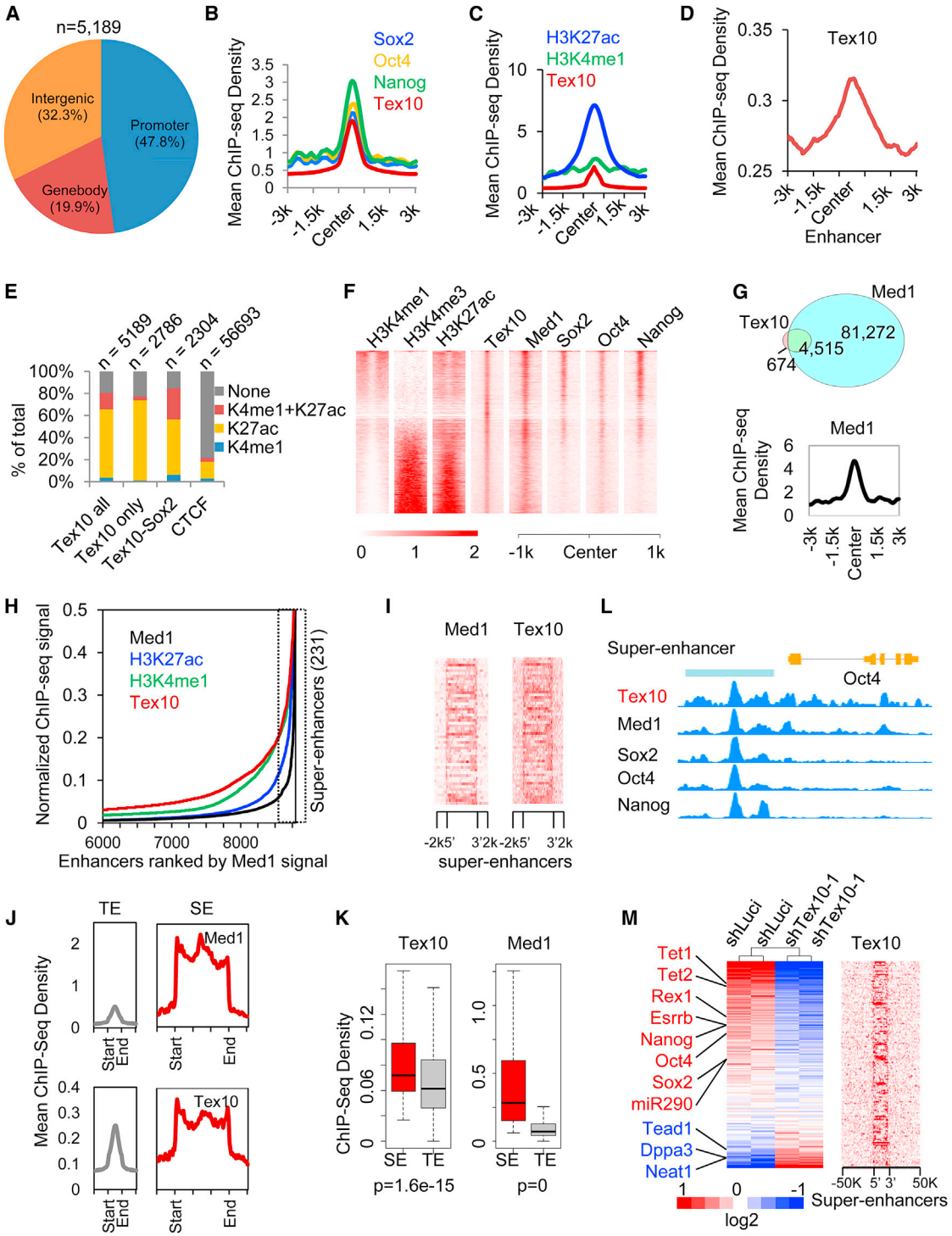

Figure 4. Tex10 Positively Regulates SE Activity with Sox2 in ESCs

(A) Distribution of Tex10 binding sites at promoter (−3 to +3 kb), gene body, and intergenic regions.

(B) Average ChIP-seq read density of Tex10, Sox2, Oct4, and Nanog near the Tex10 peak center.

(C) Average ChIP-seq read density of Tex10, H3K4me1, and H3K27ac near the Tex10 peak center.

(D) Tex10 binding regions are enriched for enhancers.

(E) Histograms showing percentage of genomic regions in ESC enhancer and Tex10 (only or shared with Sox2) and CTCF ChIP-seq peaks overlapping with H3K4me1 (K4me1), H3K27ac (K27ac), or both (K4me1+K27ac) peaks.

(F) Heatmaps of Tex10 binding loci are sorted by the enhancer mark H3K4me1 and the active promoter mark H3K4me3. H3K27ac is an active mark for both enhancers and promoters. ESC-specific enhancers are co-bound by Sox2, Oct4, Nanog, and Med1.

(legend continued on next page)

Tex10 in regulating ESC enhancer activity (see below). We sorted Tex10 peaks by H3K4me1 and H3K4me3 to distinguish enhancers from promoters, and we found that the majority of Tex10 enhancers and few Tex10 promoters are targeted by OSN (Figures 4F and S4H), reinforcing the notion that Tex10 may contribute to Sox2 functions in regulating ESC-specific enhancers. Consistent with this, the genes near Tex10 enhancers have higher expression than non-enhancer-associated genes or the genes near enhancers regardless of Tex10 binding (Figure S4I), and *Tex10* knockdown reduced the expression of the majority of Tex10 enhancer-associated genes (Figure S4J).

ESC SEs are part of ESC-specific enhancers and have a larger size, an increased ability to activate transcription, and heightened sensitivity to perturbation as compared to TEs. They are also enriched for Med1 and cell-type-specific TFs, such as OSN in ESCs (Whyte et al., 2013). The close relationship of Tex10 with OSN and Med1 in target gene occupancy (Figures 4F and S4F) prompted us to investigate potential functions of Tex10 in regulating SE activity. Previous studies identified 231 SEs according to the density of Med1 in ESCs (Whyte et al., 2013). We found that 4,515 (87%) of Tex10 binding peaks, including the majority of promoters and enhancers, are also occupied by Med1 (Figures 4F and 4G and S4K). Like Med1, Tex10 is also enriched in the regions of ESC SEs (Figures 4H and 4I) and has a significantly stronger density in SEs than in TEs (Figures 4J–4L and S4M). Correspondingly, comparison of the expression changes between SE- and TE-associated genes upon *Tex10* knockdown revealed that SE-associated genes are more sensitive to *Tex10* depletion than TE-associated genes are (Figure S4L). To address how Tex10 may regulate the expression of SE-associated genes, we selected genes closest to the SEs and examined their expression using RNA-seq data (Figure 2F). Predictably, we observed that expression of most Tex10 SE-associated genes was downregulated after *Tex10* knockdown (Figure 4M). We further employed a luciferase reporter assay whereby the *luciferase* gene is driven by the ESC-specific enhancer within the well-known SE in the *Nanog* locus, and we confirmed that Tex10 can further enhance Oct4- and Sox2-mediated enhancer activity (Figure S4M). Together our data establish Tex10 as a positive regulator of SE activity in ESCs.

Tex10 Regulates Epigenetic Modifications and eRNA Transcription of SEs

We explored molecular mechanisms by which Tex10 positively controls SE activity. Enhancer elements are pre-marked with H3K4me1 followed by H3K27ac modification to generate an open chromatin conformation for multi-factor co-occupancy (Calo and Wysocka, 2013). Although Tex10 was reported to be co-purified with MLL1/MLL complex in HeLa cells (Dou et al., 2005), we did not identify MLL components in the Tex10 interactome in ESCs (data not shown). In addition, we detected neither global expression (Figure 5A) nor locus-specific H3K4me1 enrichment change upon *Tex10* depletion (data not shown) within the time window when ESCs still maintained undifferentiated morphology and had minimal alteration of Oct4 and Sox2 expression under reduced Tex10 expression (Figure S5A). In contrast, we found that *Tex10* depletion reduced enrichment of H3K27ac modifications in the SE regions of *Oct4*, *Nanog*, and *Esrrb* loci (Figure 5B) in the presence of overall normal expression levels of H3K27ac (Figure 5A), suggesting that Tex10 may regulate SE activity mainly through modulating histone acetylation. In line with this, we found that p300, the H3K27 acetyltransferase that is enriched at enhancer regions in ESCs (Chen et al., 2008), is also highly enriched at Tex10 binding regions (Figure 5C), and that depletion of *Tex10* caused reduced binding of p300 to the SEs of *Nanog*, *Oct4*, and *Esrrb* loci (Figure 5D) without altering overall p300 expression (Figure 5A). Our data suggest that Tex10 may recruit p300 to the enhancer regions to establish H3K27 acetylation and regulate SE activity.

To further understand how Tex10-mediated p300 action on H3K27 acetylation and the resulting open chromatin of ESC enhancers may lead to target gene regulation, we asked what other Tex10 cofactors and/or epigenetic regulators may be recruited by Tex10 to ESC enhancers for transcriptional activation of enhancer-associated genes. To this end, we biochemically purified Tex10-interacting proteins in ESCs using the SILAC (stable isotope labeling by amino acids in cell culture) system coupled with IP-MS (see Supplemental Experimental Procedures for details) and identified both Tet1 and Tet2 as partners of Tex10 (Figures S5B and S5C). Further purification of Tet1 protein complexes using SILAC IP-MS in ESCs also identified Tex10 (Figure S5D). The Tex10-Tet1 interaction was further confirmed by co-IP (Figure 5E). Like Tet1 (Wu et al., 2011), Tex10 peaks are also highly enriched for CpG islands (Figure S5E). Interestingly, Tet1 is also abundant in SE regions (Figure 5F), and Tex10, Sox2, and Tet1 co-binding targets are more enriched at enhancers than promoters and other regions (Figure S5F). Furthermore, we found that ~75% of Tex10 binding peaks are also occupied by Tet1 (Figure S5G), supporting the physical and functional connection between Tex10 and Tet1.

SEs are reported to be hypomethylated with Tet1 occupancy (Pulakanti et al., 2013) and the enrichment of active enhancer

(G) Tex10 shares the majority of its targets with Med1.
(H) Distribution of Tex10, Med1, H3K4me1, and H3K27ac normalized ChIP-seq density across a subset of 8,794 ESC enhancers. For each ChIP-seq data point, we normalized the plot by dividing the ChIP-seq signals by the maximum signals individually, and we sorted them in an ascending order.
(I) The heatmap of Tex10 and Med1 intensity at 231 ESC SEs.
(J) The heatmaps of Med1 and Tex10 both show that they are enriched in SE regions.
(K) Box plot of Tex10 and Med1 ChIP-seq density (reads per million reads per base) at the SE and TE regions. Box plot whiskers extend to 1.5× the interquartile range. p values were calculated using a two-tailed t test.
(L) ChIP-seq binding profiles (reads per million per base pair) for the Tex10 and ESC TFs Oct4, Sox2, and Nanog (OSN) and Med1 at the *Oct4* locus in ESCs. Gene models are depicted above the binding profiles. SE bar and scale bar are depicted above the binding profiles.
(M) Relative expression of SE-associated genes in *Tex10*-depleted ESCs compared with *luciferase* knockdown ESCs. The genes that are closest to SEs were selected. The scale represents fold changes.
See also Figure S4.

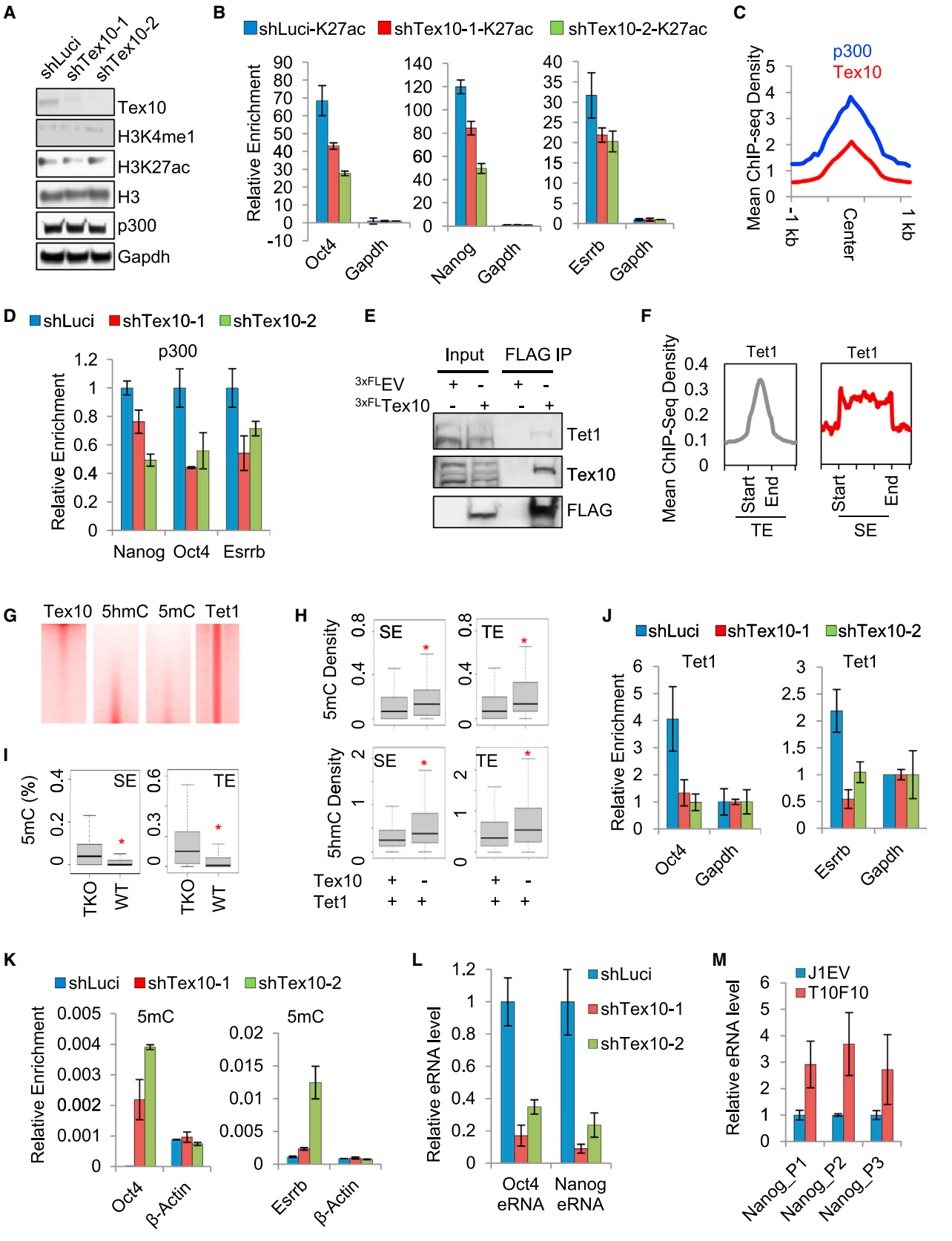

(legend on next page)

histone marks and DNA methylation density are anti-correlated (Stadler et al., 2011). Currently, whether and how Tet1 may mediate enhancer DNA demethylation and contribute to SE activity in ESCs are not well defined. We thus explored the possibility that Tet1 may cooperate with Tex10 and Sox2 in modulating the DNA methylation status of enhancer elements. We examined the levels of methylcytosine (5mC) and hydroxymethylcytosine (5hmC) at Tex10 peaks, and we found that Tex10 peaks are enriched for Tet1 but devoid of 5hmC and 5mC (Figure S5H). We also examined the levels of 5mC and 5hmC at Tet1 peaks sorted by Tex10 intensity and again found that Tex10 peaks are devoid of 5hmC and 5mC (Figure 5G). These data indicate that Tex10-bound DNA regions are unmethylated. Interestingly, we noticed that Sox2 and Tet1 shared peaks are enriched for either Tex10 or 5hmC (Figure S5I) and that Tet1 binding SEs and TEs have significantly lower levels of 5mC and 5hmC when they are also targeted by Tex10 (Figure 5H). Depletion of Tet proteins significantly induced 5mC accumulations at Tet1/Tex10 co-binding SE and TE regions (Figure 5I). These analyses suggest that Tex10 may induce active DNA demethylation through facilitating DNA demethylase Tet1 accessibility to Tex10/Sox2 co-bound targets. Supporting this, we found that depletion of *Tex10* reduced the binding of Tet1, whose expression is maintained within the time window tested (Figure S5A), to the SE regions of *Oct4* and *Esrrb* loci (Figure 5J) with a concomitant increase in 5mC enrichment at the same regions (Figure 5K). Together, these results establish a Tex10-dependent function of Tet1 in binding to Tex10-occupied SEs and modulating methylation status of SEs.

To correlate DNA demethylation of SEs with their transcriptional activities, we examined transcription of eRNAs associated with SEs based on the findings that (1) eRNAs are transcribed in SEs (Hnisz et al., 2013); (2) eRNAs arise from hypomethylated, Tet1-occupied genomic regions (Pulakanti et al., 2013); and (3) eRNAs promote associated mRNA transcription by establishing chromatin accessibility and tethering enhancer activity to the transcriptional apparatus (Mousavi et al., 2013). We first examined transcription of SE-associated eRNAs before and after *Tex10* knockdown. We found that *Tex10* knockdown decreased the expression of a number of previously reported eRNAs in ESCs (Pulakanti et al., 2013) including those associated with *Oct4* and *Nanog* (Figures 5L and S5J). Conversely, ectopic expression of *Tex10* increased transcription of those eRNAs (Figures 5M and S5K).

Collectively, our studies establish Tex10 as a major player in the ESC enhanceosome assembly that regulates the SE activity and eRNA transcription by cooperating with p300 and Tet1 to control the histone acetylation and DNA hypomethylation of SEs, respectively. Our results on Tet1's participation in the Sox2-guided ESC enhanceosome assembly via its Tex10 association sheds new light on our understanding of Tet proteins in modulating enhancer activity in ESCs (Hon et al., 2014; Lu et al., 2014) (see more in Discussion).

Sox2 Directs Tex10 to a Subset of Shared ESC-Specific SEs

Because Tex10 and Sox2 physically interact (Figure 1) and share many targets at ESC-specific enhancer regions (Figure 6A), and because a Sox2-dependent function of Tex10 in establishing both active enhancer marks (H3K4me1+H3K27ac) was observed (Figure 4E), we hypothesized that Sox2 may recruit Tex10 to these enhancers. To test this hypothesis, we created an ESC line (2TST10) by introducing a constitutive 3×FLAG-tagged *Tex10* transgene into the 2TS22C ESC line (Masui et al., 2007) that has both endogenous *Sox2* alleles removed and replaced with a doxycycline (Dox) suppressible *Sox2* transgene for stem cell maintenance (Figure 6B). After 14 hr of Dox treatment, Sox2 protein was depleted to a low level, whereas Oct4 and Nanog are maintained together with constitutive FLAG-tagged Tex10 protein expression (Figure 6C). ChIP-qPCR was performed to analyze Tex10 binding to the shared target loci upon Dox treatment (i.e., depletion of *Sox2*), which revealed that Tex10 binding decreased significantly after Dox treatment at *Nanog*, *Oct4*, and *Sox2* loci (Figures 6D–6F) despite its normal expression (Figure 6C). In contrast, Tex10 binding is not affected by *Sox2* depletion in the Tex10-only genomic loci (Figures S6A–S6C). These data indicate that Sox2 directs Tex10 to a subset of shared ESC SEs in controlling their activities.

Functional Conservation of Human TEX10 in Pluripotency and Reprogramming

To further address whether Tex10's functions in pluripotency and reprogramming are evolutionally conserved, we performed

Figure 5. Tex10 Regulates the Modifications and eRNA Transcription of SEs

(A) Protein expression levels of Tex10, H3K4me1, H3K27ac, H3, p300, and Gapdh after 68 hr of Tex10 knockdown.

(B) Impact of *Tex10* depletion on H3K27ac occupancy at *Oct4*, *Nanog*, and *Esrrb* SEs. CCE ESCs were treated with shRNA against *Tex10* for 68 hr to induce *Tex10* depletion, and H3K27ac occupancy was determined by ChIP-qPCR. Data are presented as mean ± SEM (n = 3).

(C) Average ChIP-seq read density of Tex10 and p300 near the Tex10 peak center.

(D) Impact of *Tex10* depletion on p300 occupancy at *Oct4*, *Nanog*, and *Esrrb* SEs. CCE ESCs were treated with shRNA against *Tex10* for 68 hr to induce Tex10 depletion, and p300 occupancy was determined by ChIP-qPCR. Data are presented as mean ± SEM (n = 3).

(E) Validation of the Tex10-Tet1 interaction by co-IP in ESCs expressing 3×FLAg-tagged Tex10.

(F) Metagenes of Tet1 ChIP-seq density (reads per million per base pair) across the 8,563 TEs and the 231 SEs.

(G) Heatmaps showing that Tet1 peaks are separated by Tex10 and 5hmC/5mC enrichment.

(H) Density of 5mC and 5hmC at Tet1 binding SE or TE regions.

(I) 5mC percentages of Tet1/Tex10 co-binding SEs or TEs at WT and TKO (*Tet1/2/3* triple knockout) ESCs.

(J) Tet1 enrichment in *Oct4* and *Esrrb* SE regions after 68 hr of *Tex10* knockdown. Data are presented as mean ± SEM (n = 3).

(K) 5mC enrichment in *Oct4* and *Esrrb* SE regions after 68 hr of *Tex10* knockdown. Data are presented as mean ± SEM (n = 3).

(L) eRNA expression of *Oct4* and *Nanog* SEs after 4 days of *Tex10* knockdown. Data are presented as mean ± SEM (n = 3).

(M) eRNA expression of *Nanog* SE after overexpression of *Tex10*. Data are presented as mean ± SEM (n = 3).

See also Figure S5.

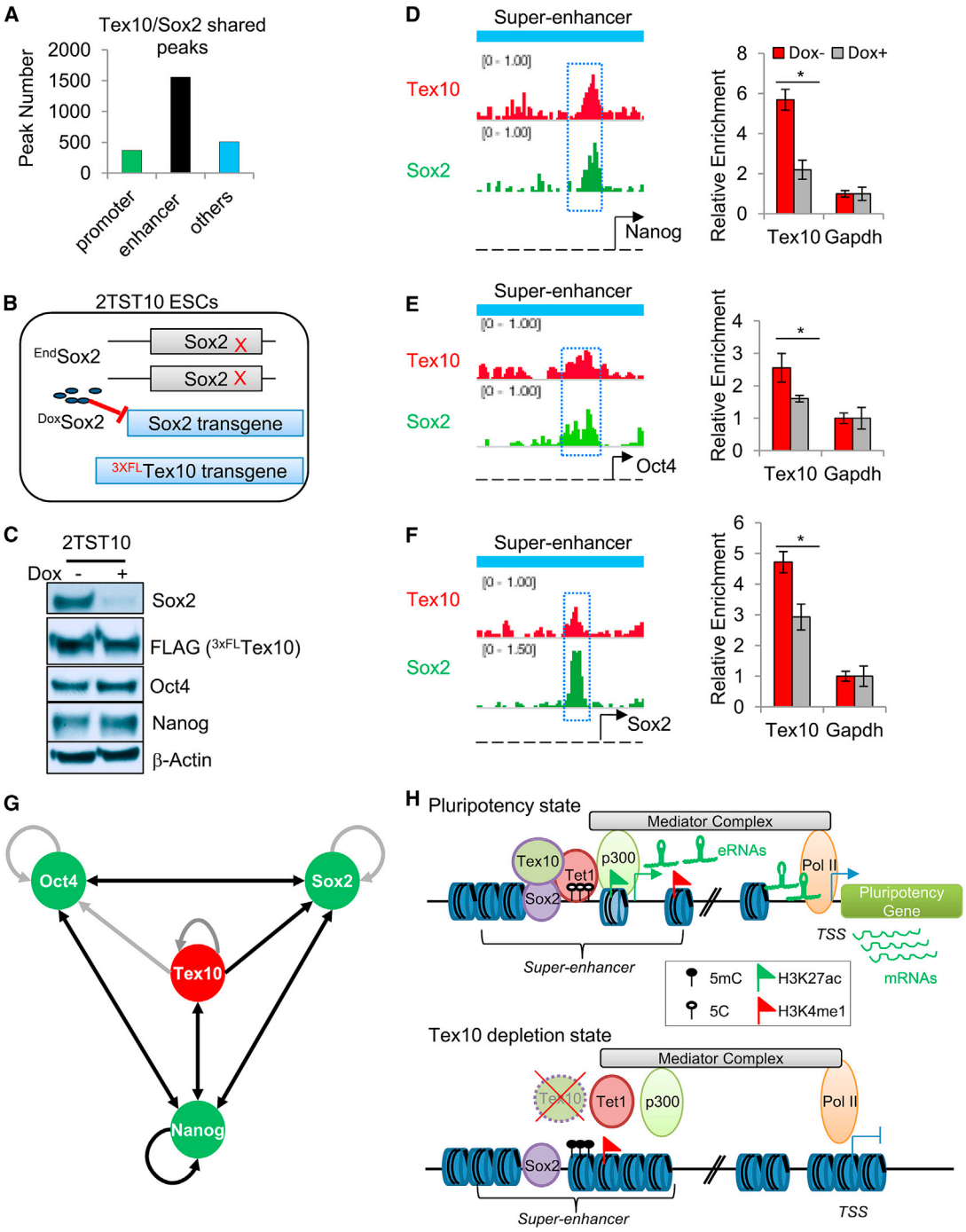

Figure 6. Sox2 Recruits Tex10 to a Subset of SEs in ESCs

(A) Most Tex10/Sox2 shared peaks are enriched at enhancers.

(B) Schematic overview of the 2TST10 ESCs. ^{End}*Sox2*, endogenous *Sox2* allele; ^{Dox}*Sox2*, doxycycline repressible *Sox2* allele.

(C) Protein levels after 14 hr of Dox treatment in 2TST10 ESCs.

(D–F) Dox treatment decreased the enrichment of Tex10 at the SEs of *Nanog* (D), *Oct4* (E), and *Sox2* (F). Data are presented as mean ± SEM (n = 3).

(G) Tex10 is integrated to the core pluripotency network through protein-protein or protein-DNA interactions. The gray arrows indicate protein-DNA interactions only, whereas the black arrows indicate both protein-protein and protein-DNA interactions.

(H) A model depicting functions of Tex10 on the regulation of SE-associated genes. In the pluripotency state, Tex10 co-occupies with Sox2/Med1 and recruits Tet1 and p300 to the SEs for DNA demethylation and histone acetylation, leading to active eRNA/mRNA transcription. In *Tex10*-depleted cells, Tet1 and p300 cannot be recruited to the SEs, resulting in DNA hypermethylation and reduced H3K27ac enrichment at SEs and, consequently, the loss of SE activity and pluripotency gene expression. For simplicity, other pluripotency factors known to be present in ESC SEs such as Nanog, Oct4, and Tet2 are omitted in the illustration.

See also Figure S6.

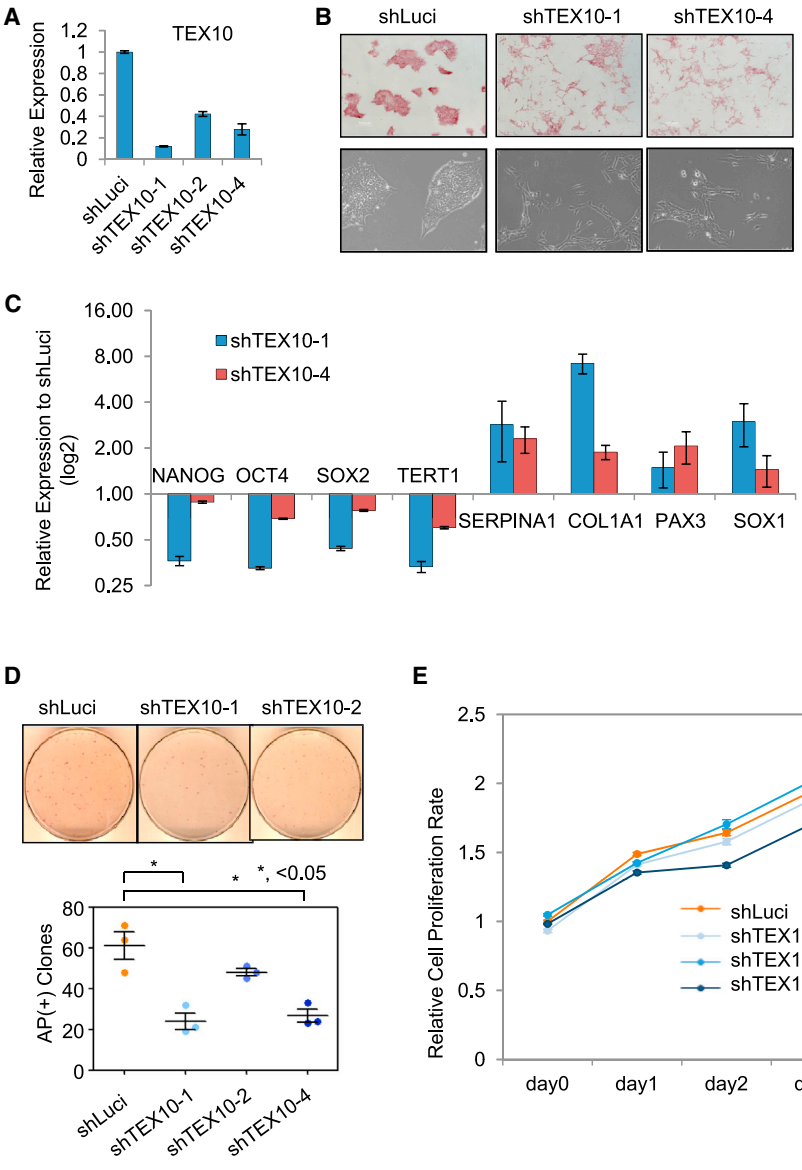

Figure 7. Human TEX10 Plays Critical Roles in Human Pluripotency and Reprogramming

(A) Knockdown efficiency of the shRNAs against human *TEX10* 4 days after *TEX10* knockdown. Data are presented as mean ± SEM (n = 3).

(B) Morphology of hESCs upon *luciferase* and *TEX10* knockdown. Top, AP staining of hESCs; bottom, phase contrast microscopy of hESCs.

(C) Expression of human pluripotency and lineage markers in *luciferase* and *TEX10* knockdown hESCs. Data are presented as mean ± SEM (n = 3).

(D) Reprogramming efficiency of the human BJ cells with *luciferase* or *TEX10* depletion. Representative AP-positive iPSC colonies and quantitative data from three different experiments were shown on top and bottom panels, respectively.

(E) Proliferation of human BJ cells after *TEX10* knockdown.

loss-of-function studies of human *TEX10* on hESC maintenance and human iPSC (hiPSC) generation. Using independent shRNAs targeting human *TEX10* (Figure 7A), we found that *TEX10* depletion led to differentiation of hESCs with reduced AP staining (Figure 7B), concomitant downregulation of pluripotency genes *NANOG*, *OCT4*, *SOX2*, and *TERT1*, and upregulation of lineage-specific genes (Figure 7C). These data demonstrate a critical role of TEX10 for hESC maintenance. To test whether TEX10 is also important for the establishment of human pluripotency, we performed human iPSC generation from BJ cells with conventional Yamanaka reprogramming factors. We found that *TEX10* depletion resulted in a decreased reprogramming efficiency (Figure 7D) with minimal effects on BJ cell proliferation (Figure 7E), supporting the functional significance of human TEX10 in the establishment of human pluripotency.

Together these data establish the evolutionally conserved function of Tex10/TEX10 in controlling both stem cell pluripotency and somatic cell reprogramming.

DISCUSSION

Our study uncovered Sox2-dependent functions of Tex10 in controlling ESC-specific enhancer and particularly SE activity through recruitment of the histone acetyltransferase p300 and the DNA demethylase Tet1 for the transcriptional regulation of SE-associated eRNA and mRNA expression. Although there likely exist Sox2-independent functions of Tex10 in promoter regulation (Figures 4A and S4H), we primarily focused on dissecting the potential contribution of Tex10 to Sox2-guided enhanceosome assembly and in particular, SEs, due to their prominent roles in maintaining pluripotency. We have provided multiple lines of evidence integrating Tex10 into the core pluripotency network (Figure 6G) for epigenetic control of SE activity and ESC identity: Tex10 orchestrates histone H3K27 acetylation, DNA demethylation, and eRNA transcription, as succinctly summarized in a model (Figure 6H) and further discussed below.

First, our transcriptome (Figure 2) and genomic binding (Figures 4 and S4) correlation analyses, together with the physical association (Figure 1) between Tex10 and other pluripotency factors, position Tex10 in the center of the previously defined OSN triumvirate regulatory loop controlling pluripotency (Kim et al., 2008) (Figure 6G).

Second, while ectopic Oct4 and Sox2 can modestly activate the *Nanog* enhancer in HEK293T cells devoid of endogenous Oct4 and Sox2, a further activation effect can be achieved when Tex10 is combined with Oct4 and Sox2 (Figure S4M). Our data indicate that Tex10 may function as an Oct4/Sox2 co-activator by recruiting p300 to the SEs for induction of H3K27ac (Figures 5A–5D), which leads to activated pluripotency gene expression in ESCs.

Third, we established Tex10 function in regulating enhancer activity through Tet1-mediated DNA demethylation. Studies have suggested that Tet1 and Tet2 have distinct roles in controlling enhancer activity in ESCs (Hon et al., 2014; Huang et al., 2014). It was also reported that active and initiated enhancers are predominantly hypermethylated with concomitant transcriptional downregulation of enhancer-associated genes in *Tet* TKO ESCs (Lu et al., 2014). While 5hmC is abundant at both poised and active enhancers in ESCs (Yu et al., 2012), our findings led us to hypothesize that recruitment of Tet1 by Tex10 may facilitate active DNA demethylation of SEs. Supporting this hypothesis, our data show that *Tex10* depletion reduces Tet1 binding and induces 5mC enrichment in *Oct4* and *Esrrb* enhancers in undifferentiated ESCs (Figures 5J and 5K). However, we cannot exclude the possible contribution of Tet2 to the observed SE hypomethylation due to the association of Tet2 with Tex10 (Figures S5B and S5C). Nevertheless, hypermethylation of enhancer regions alone cannot account for the loss of self-renewal and differentiation of *Tex10*-depleted ESCs (Figures 2, S2, and 7) because *Tet* TKO ESCs retain ESC characteristics (Dawlaty et al., 2014; Lu et al., 2014). Rather, our study highlights the significant role of Tex10, as a newly discovered core pluripotency factor, in orchestrating multiple epigenetic regulatory events that together control enhancer activity and pluripotent cell identity. Thus, depletion of Tex10 can lead to enhancer decommissioning through a combined action of loss of H3K27 acetylation and DNA hypermethylation, and consequently, to the derailment of the pluripotency program.

Fourth, our study identifies a critical component of the enhanceosome assembly in ESCs, namely the Sox2-Tex10-Tet1 triumvirate, that may directly contribute to the open chromatin and hypomethylation status of SEs leading to active transcription of eRNAs and mRNAs. Tex10 is a structured protein containing an Armadillo-type fold, an Armadillo-like helical, and a type 2 HEAT domain, which can be the interface for protein, DNA, and RNA binding. Such a unique structure of Tex10 may have endowed this key pluripotency factor with versatile functions in orchestrating histone acetylation, DNA demethylation, and eRNA regulation to control SE activity and pluripotent cell identity. Dissection of the structure-function relationship of Tex10 in ESCs and during reprogramming is warranted for future investigation.

Finally, the evolutionally conserved function in pluripotency and reprogramming (Figure 7) further consolidates the status of Tex10/TEX10 as a newly-arrived key player in the core pluripotency network, although the potential caveat exists that the proliferation defect of its depletion may have partly contributed to the compromised pluripotency and reprogramming. Future studies in dissecting the mechanistic action of TEX10 in human cells should shed new light on human pluripotency and provide additional means to enhance optimal maintenance/derivation of hESCs/hiPSCs for therapeutic application and regenerative medicine.

EXPERIMENTAL PROCEDURES

Additional experimental procedures are provided in the Supplemental Experimental Procedures.

Affinity Purification of Sox2 Protein Complexes in ESCs

The ESC lines of J1, BirA (containing *BirA-V5* transgene), and Sox2#7 (containing ^{FLBIO}*Sox2* and *BirA-V5* transgene) were expanded to five large square dishes (245 × 245 mm) and were used to prepare nuclear extracts as previously described (Ding et al., 2012). Three independent streptavidin (SA) and one FLAG IP, followed by MS identification, were performed as described (Costa et al., 2013; Ding et al., 2012) to identify bona fide Sox2-interacting proteins in ESCs. To further improve the quality of the interactome, we also performed endogenous Sox2 antibody-based IP in wild-type J1 ESCs followed by MS identification. Details are given in the Supplemental Experimental Procedures.

Generation of Tex10 Knockout Mouse Model

An ESC clone Tex10_AB8 harboring a LacZ knockin cassette at the Tex10 locus resulting in a knockout allele was obtained from KOMP Repository Knockout Mouse Project. To generate chimeric embryos, we injected 10–12 *Tex10* heterozygous ESCs into Balb/c (albino) E3.5 wild-type blastocysts and surgically implanted them into 2.5 dpc pseudo-pregnant Swiss Webster female mice following standard procedures. The chimeras with >50% black coat color were mated with C57Bl/6N wild-type mice to test germline transmission. Details on genotyping, staged embryo analysis, and ESC derivation are given in the Supplemental Experimental Procedures.

Mouse Embryo Collection and Microinjection

The embryo experiments were performed as previously described (Wang et al., 2014) with modifications described in the Supplemental Experimental Procedures.

ChIP Coupled with ChIP-qPCR

ChIP was performed as previously described (Lee et al., 2006).

Reprogramming Assays in Adult Neural Stem and MEF Cells

Reprogramming was performed as previously described (Costa et al., 2013).

ACCESSION NUMBERS

The accession number for the Tex10 ChIP-seq and RNA-seq data reported in this paper is GEO: GSE66736.

SUPPLEMENTAL INFORMATION

Supplemental Information for this article includes Supplemental Experimental Procedures, six figures, and eight tables and can be found with this article online at http://dx.doi.org/10.1016/j.stem.2015.04.001.

AUTHOR CONTRIBUTIONS

J.D. designed and performed experiments, analyzed data, and wrote the manuscript; X.H., N.S., D.P., and L.S. provided bioinformatics support; H.Z. and D.-F.L. helped with human ESC/iPSC assays; F.F., M.F., D.G., A.S., D.L., H.W., A.W., Y.Y., and I.R.L. provided technical assistance, reagents, and helpful discussions; P.V.S. performed the interactome analysis; K.K. helped with early embryo work and generation of the knockout mouse model; H.D. and X.S. helped with mass spectrometry; and J.W. conceived the project, designed the experiments, analyzed data, and prepared and approved the manuscript.

ACKNOWLEDGMENTS

We thank Dr. Jose Silva (United Kingdom) for the pre-iPSCs; Dr. Hitoshi Niwa (Japan) for the 2TS22C ESCs; Dr. Thamar van Dijk (The Nethelands) for Wdr18, Tex10, and Las1L plasmids; and Dr. Huck-Hui Ng (Singapore) for the *Nanog*-enhancer *luciferase* construct. Production of the knockout mouse model and injections of siRNAs in early embryos were performed in the Mouse Genetics Shared Resource Facility at the Icahn School of Medicine at Mount Sinai. This research was funded by grants from the NIH to J.W. (1R01-GM095942) and the Empire State Stem Cell Fund through New York State Department of Health (NYSTEM) to J.W. (C028103 and C028121). J.W. is a recipient of an Irma T. Hirschl and Weill-Caulier Trusts Career Scientist Award. A.S. is an awardee of the Traineeship of NIDCR-Interdisciplinary Training in Systems and Developmental Biology and Birth Defects (T32HD075735).

Received: January 13, 2015
Revised: March 25, 2015
Accepted: April 3, 2015
Published: April 30, 2015

REFERENCES

Ang, Y.S., Tsai, S.Y., Lee, D.F., Monk, J., Su, J., Ratnakumar, K., Ding, J., Ge, Y., Darr, H., Chang, B., et al. (2011). Wdr5 mediates self-renewal and reprogramming via the embryonic stem cell core transcriptional network. Cell *145*, 183–197.

Ben-Porath, I., Thomson, M.W., Carey, V.J., Ge, R., Bell, G.W., Regev, A., and Weinberg, R.A. (2008). An embryonic stem cell-like gene expression signature in poorly differentiated aggressive human tumors. Nat. Genet. *40*, 499–507.

Buecker, C., Srinivasan, R., Wu, Z., Calo, E., Acampora, D., Faial, T., Simeone, A., Tan, M., Swigut, T., and Wysocka, J. (2014). Reorganization of enhancer patterns in transition from naive to primed pluripotency. Cell Stem Cell *14*, 838–853.

Buganim, Y., Faddah, D.A., Cheng, A.W., Itskovich, E., Markoulaki, S., Ganz, K., Klemm, S.L., van Oudenaarden, A., and Jaenisch, R. (2012). Single-cell expression analyses during cellular reprogramming reveal an early stochastic and a late hierarchic phase. Cell *150*, 1209–1222.

Calo, E., and Wysocka, J. (2013). Modification of enhancer chromatin: what, how, and why? Mol. Cell *49*, 825–837.

Card, D.A., Hebbar, P.B., Li, L., Trotter, K.W., Komatsu, Y., Mishina, Y., and Archer, T.K. (2008). Oct4/Sox2-regulated miR-302 targets cyclin D1 in human embryonic stem cells. Mol. Cell. Biol. *28*, 6426–6438.

Castle, C.D., Cassimere, E.K., and Denicourt, C. (2012). LAS1L interacts with the mammalian Rix1 complex to regulate ribosome biogenesis. Mol. Biol. Cell *23*, 716–728.

Chen, X., Xu, H., Yuan, P., Fang, F., Huss, M., Vega, V.B., Wong, E., Orlov, Y.L., Zhang, W., Jiang, J., et al. (2008). Integration of external signaling pathways with the core transcriptional network in embryonic stem cells. Cell *133*, 1106–1117.

Chen, J., Zhang, Z., Li, L., Chen, B.C., Revyakin, A., Hajj, B., Legant, W., Dahan, M., Lionnet, T., Betzig, E., et al. (2014). Single-molecule dynamics of enhanceosome assembly in embryonic stem cells. Cell *156*, 1274–1285.

Costa, Y., Ding, J., Theunissen, T.W., Faiola, F., Hore, T.A., Shliaha, P.V., Fidalgo, M., Saunders, A., Lawrence, M., Dietmann, S., et al. (2013). NANOG-dependent function of TET1 and TET2 in establishment of pluripotency. Nature *495*, 370–374.

Creyghton, M.P., Cheng, A.W., Welstead, G.G., Kooistra, T., Carey, B.W., Steine, E.J., Hanna, J., Lodato, M.A., Frampton, G.M., Sharp, P.A., et al. (2010). Histone H3K27ac separates active from poised enhancers and predicts developmental state. Proc. Natl. Acad. Sci. USA *107*, 21931–21936.

Dawlaty, M.M., Breiling, A., Le, T., Barrasa, M.I., Raddatz, G., Gao, Q., Powell, B.E., Cheng, A.W., Faull, K.F., Lyko, F., and Jaenisch, R. (2014). Loss of Tet enzymes compromises proper differentiation of embryonic stem cells. Dev. Cell *29*, 102–111.

Ding, J., Xu, H., Faiola, F., Ma'ayan, A., and Wang, J. (2012). Oct4 links multiple epigenetic pathways to the pluripotency network. Cell Res. *22*, 155–167.

Dos Santos, R.L., Tosti, L., Radzisheuskaya, A., Caballero, I.M., Kaji, K., Hendrich, B., and Silva, J.C. (2014). MBD3/NuRD Facilitates Induction of Pluripotency in a Context-Dependent Manner. Cell Stem Cell *15*, 102–110.

Dou, Y., Milne, T.A., Tackett, A.J., Smith, E.R., Fukuda, A., Wysocka, J., Allis, C.D., Chait, B.T., Hess, J.L., and Roeder, R.G. (2005). Physical association and coordinate function of the H3 K4 methyltransferase MLL1 and the H4 K16 acetyltransferase MOF. Cell *121*, 873–885.

Fanis, P., Gillemans, N., Aghajanirefah, A., Pourfarzad, F., Demmers, J., Esteghamat, F., Vadlamudi, R.K., Grosveld, F., Philipsen, S., and van Dijk, T.B. (2012). Five friends of methylated chromatin target of protein-arginine-methyltransferase[prmt]-1 (chtop), a complex linking arginine methylation to desumoylation. Mol. Cell. Proteomics *11*, 1263–1273.

Fong, Y.W., Ho, J.J., Inouye, C., and Tjian, R. (2014). The dyskerin ribonucleoprotein complex as an OCT4/SOX2 coactivator in embryonic stem cells. eLife *3*, 3.

Gagliardi, A., Mullin, N.P., Ying Tan, Z., Colby, D., Kousa, A.I., Halbritter, F., Weiss, J.T., Felker, A., Bezstarosti, K., Favaro, R., et al. (2013). A direct physical interaction between Nanog and Sox2 regulates embryonic stem cell self-renewal. EMBO J. *32*, 2231–2247.

Gao, Z., Cox, J.L., Gilmore, J.M., Ormsbee, B.D., Mallanna, S.K., Washburn, M.P., and Rizzino, A. (2012). Determination of protein interactome of transcription factor Sox2 in embryonic stem cells engineered for inducible expression of four reprogramming factors. J. Biol. Chem. *287*, 11384–11397.

Gontan, C., Güttler, T., Engelen, E., Demmers, J., Fornerod, M., Grosveld, F.G., Tibboel, D., Görlich, D., Poot, R.A., and Rottier, R.J. (2009). Exportin 4 mediates a novel nuclear import pathway for Sox family transcription factors. J. Cell Biol. *185*, 27–34.

Hindley, C., and Philpott, A. (2013). The cell cycle and pluripotency. Biochem. J. *451*, 135–143.

Hnisz, D., Abraham, B.J., Lee, T.I., Lau, A., Saint-André, V., Sigova, A.A., Hoke, H.A., and Young, R.A. (2013). Super-Enhancers in the Control of Cell Identity and Disease. Cell *155*, 934–947.

Hon, G.C., Song, C.X., Du, T., Jin, F., Selvaraj, S., Lee, A.Y., Yen, C.A., Ye, Z., Mao, S.Q., Wang, B.A., et al. (2014). 5mC oxidation by Tet2 modulates enhancer activity and timing of transcriptome reprogramming during differentiation. Mol. Cell *56*, 286–297.

Hu, G., and Wade, P.A. (2012). NuRD and pluripotency: a complex balancing act. Cell Stem Cell *10*, 497–503.

Huang, X., and Wang, J. (2014). The extended pluripotency protein interactome and its links to reprogramming. Curr. Opin. Genet. Dev. *28*, 16–24.

Huang, Y., Chavez, L., Chang, X., Wang, X., Pastor, W.A., Kang, J., Zepeda-Martínez, J.A., Pape, U.J., Jacobsen, S.E., Peters, B., and Rao, A. (2014). Distinct roles of the methylcytosine oxidases Tet1 and Tet2 in mouse embryonic stem cells. Proc. Natl. Acad. Sci. USA *111*, 1361–1366.

Kagey, M.H., Newman, J.J., Bilodeau, S., Zhan, Y., Orlando, D.A., van Berkum, N.L., Ebmeier, C.C., Goossens, J., Rahl, P.B., Levine, S.S., et al. (2010). Mediator and cohesin connect gene expression and chromatin architecture. Nature *467*, 430–435.

Kim, J., Chu, J., Shen, X., Wang, J., and Orkin, S.H. (2008). An extended transcriptional network for pluripotency of embryonic stem cells. Cell *132*, 1049–1061.

Lam, C.S., Mistri, T.K., Foo, Y.H., Sudhaharan, T., Gan, H.T., Rodda, D., Lim, L.H., Chou, C., Robson, P., Wohland, T., and Ahmed, S. (2012). DNA-dependent Oct4-Sox2 interaction and diffusion properties characteristic of the pluripotent cell state revealed by fluorescence spectroscopy. Biochem. J. *448*, 21–33.

Lam, M.T., Li, W., Rosenfeld, M.G., and Glass, C.K. (2014). Enhancer RNAs and regulated transcriptional programs. Trends Biochem. Sci. *39*, 170–182.

Lee, T.I., Johnstone, S.E., and Young, R.A. (2006). Chromatin immunoprecipitation and microarray-based analysis of protein location. Nat. Protoc. *1*, 729–748.

Lee, D.F., Su, J., Ang, Y.S., Carvajal-Vergara, X., Mulero-Navarro, S., Pereira, C.F., Gingold, J., Wang, H.L., Zhao, R., Sevilla, A., et al. (2012). Regulation of embryonic and induced pluripotency by aurora kinase-p53 signaling. Cell Stem Cell *11*, 179–194.

Lu, F., Liu, Y., Jiang, L., Yamaguchi, S., and Zhang, Y. (2014). Role of Tet proteins in enhancer activity and telomere elongation. Genes Dev. *28*, 2103–2119.

Mallanna, S.K., Ormsbee, B.D., Iacovino, M., Gilmore, J.M., Cox, J.L., Kyba, M., Washburn, M.P., and Rizzino, A. (2010). Proteomic analysis of Sox2-associated proteins during early stages of mouse embryonic stem cell differentiation identifies Sox21 as a novel regulator of stem cell fate. Stem Cells *28*, 1715–1727.

Masui, S., Nakatake, Y., Toyooka, Y., Shimosato, D., Yagi, R., Takahashi, K., Okochi, H., Okuda, A., Matoba, R., Sharov, A.A., et al. (2007). Pluripotency governed by Sox2 via regulation of Oct3/4 expression in mouse embryonic stem cells. Nat. Cell Biol. *9*, 625–635.

Meissner, A., Eminli, S., and Jaenisch, R. (2009). Derivation and manipulation of murine embryonic stem cells. Methods in Mol. Biol. *482*, 3–19.

Mousavi, K., Zare, H., Dell'orso, S., Grontved, L., Gutierrez-Cruz, G., Derfoul, A., Hager, G.L., and Sartorelli, V. (2013). eRNAs promote transcription by establishing chromatin accessibility at defined genomic loci. Mol. Cell *51*, 606–617.

Pardo, M., Lang, B., Yu, L., Prosser, H., Bradley, A., Babu, M.M., and Choudhary, J. (2010). An expanded Oct4 interaction network: implications for stem cell biology, development, and disease. Cell Stem Cell *6*, 382–395.

Polo, J.M., Anderssen, E., Walsh, R.M., Schwarz, B.A., Nefzger, C.M., Lim, S.M., Borkent, M., Apostolou, E., Alaei, S., Cloutier, J., et al. (2012). A molecular roadmap of reprogramming somatic cells into iPS cells. Cell *151*, 1617–1632.

Pulakanti, K., Pinello, L., Stelloh, C., Blinka, S., Allred, J., Milanovich, S., Kiblawi, S., Peterson, J., Wang, A., Yuan, G.C., and Rao, S. (2013). Enhancer transcribed RNAs arise from hypomethylated, Tet-occupied genomic regions. Epigenetics *8*, 1303–1320.

Rais, Y., Zviran, A., Geula, S., Gafni, O., Chomsky, E., Viukov, S., Mansour, A.A., Caspi, I., Krupalnik, V., Zerbib, M., et al. (2013). Deterministic direct reprogramming of somatic cells to pluripotency. Nature *502*, 65–70.

Schoeftner, S., Scarola, M., Comisso, E., Schneider, C., and Benetti, R. (2013). An Oct4-pRb axis, controlled by MiR-335, integrates stem cell self-renewal and cell cycle control. Stem Cells *31*, 717–728.

Silva, J., Barrandon, O., Nichols, J., Kawaguchi, J., Theunissen, T.W., and Smith, A. (2008). Promotion of reprogramming to ground state pluripotency by signal inhibition. PLoS Biol. *6*, e253.

Stadler, M.B., Murr, R., Burger, L., Ivanek, R., Lienert, F., Schöler, A., van Nimwegen, E., Wirbelauer, C., Oakeley, E.J., Gaidatzis, D., et al. (2011). DNA-binding factors shape the mouse methylome at distal regulatory regions. Nature *480*, 490–495.

Tang, F., Barbacioru, C., Nordman, E., Bao, S., Lee, C., Wang, X., Tuch, B.B., Heard, E., Lao, K., and Surani, M.A. (2011). Deterministic and stochastic allele specific gene expression in single mouse blastomeres. PLoS ONE *6*, e21208.

van den Berg, D.L., Snoek, T., Mullin, N.P., Yates, A., Bezstarosti, K., Demmers, J., Chambers, I., and Poot, R.A. (2010). An Oct4-centered protein interaction network in embryonic stem cells. Cell Stem Cell *6*, 369–381.

Wang, J., Rao, S., Chu, J., Shen, X., Levasseur, D.N., Theunissen, T.W., and Orkin, S.H. (2006). A protein interaction network for pluripotency of embryonic stem cells. Nature *444*, 364–368.

Wang, L., Du, Y., Ward, J.M., Shimbo, T., Lackford, B., Zheng, X., Miao, Y.L., Zhou, B., Han, L., Fargo, D.C., et al. (2014). INO80 facilitates pluripotency gene activation in embryonic stem cell self-renewal, reprogramming, and blastocyst development. Cell Stem Cell *14*, 575–591.

Whyte, W.A., Orlando, D.A., Hnisz, D., Abraham, B.J., Lin, C.Y., Kagey, M.H., Rahl, P.B., Lee, T.I., and Young, R.A. (2013). Master transcription factors and mediator establish super-enhancers at key cell identity genes. Cell *153*, 307–319.

Wu, H., D'Alessio, A.C., Ito, S., Xia, K., Wang, Z., Cui, K., Zhao, K., Sun, Y.E., and Zhang, Y. (2011). Dual functions of Tet1 in transcriptional regulation in mouse embryonic stem cells. Nature *473*, 389–393.

Yu, M., Hon, G.C., Szulwach, K.E., Song, C.X., Zhang, L., Kim, A., Li, X., Dai, Q., Shen, Y., Park, B., et al. (2012). Base-resolution analysis of 5-hydroxymethylcytosine in the mammalian genome. Cell *149*, 1368–1380.

Zhang, X., Neganova, I., Przyborski, S., Yang, C., Cooke, M., Atkinson, S.P., Anyfantis, G., Fenyk, S., Keith, W.N., Hoare, S.F., et al. (2009). A role for NANOG in G1 to S transition in human embryonic stem cells through direct binding of CDK6 and CDC25A. J. Cell Biol. *184*, 67–82.

Zhang, Q., Shalaby, N.A., and Buszczak, M. (2014). Changes in rRNA transcription influence proliferation and cell fate within a stem cell lineage. Science *343*, 298–301.